Research Article

Formulation of a Novel Oxybenzone-Loaded Nanostructured Lipid Carriers (NLCs)

Rania A. Sanad,[1] Nevine Shawky AbdelMalak,[2,3] Tahany S. elBayoomy,[1] and Alia A. Badawi[2]

Abstract. The objective of the current study was to formulate oxybenzone into nanostructured lipid carriers (NLCs) to enhance its sunscreening efficacy and safety. NLCs of oxybenzone were prepared by the solvent diffusion method. A complete 2^3 factorial design was used for the evaluation of the prepared oxybenzone NLCs. The study design involves the investigation of the effect of three independent variables namely liquid lipid type (Miglyol 812 and oleic acid), liquid lipid concentration (15% and 30%), and oxybenzone concentration (5% and 10% with respect to total lipids) on the particle size (p.s.) , the entrapment efficiency (EE%) and the *in vitro* drug release after 8 h. The prepared NLCs were spherical in overall shape and were below 0.8 μm. Miglyol 812 and 30% liquid lipid were found to significantly decrease the p.s. and increase the EE% when compared to oleic acid and 15% liquid lipid. Increasing oxybenzone concentration increased significantly the p.s. but did not affect the EE%. NLCs prepared using Miglyol 812, 15% liquid lipid, and 10% oxybenzone showed slower drug release when compared to those prepared using oleic acid, 30% liquid lipid, and 5% oxybenzone, respectively. The candidate oxybenzone-loaded NLC dispersion was then formulated into gel. The incorporation of oxybenzone into NLCs greatly increased the *in vitro* sun protection factor and erythemal UVA protection factor of oxybenzone more than six- and eightfold, respectively, while providing the advantage of overcoming side effects of free oxybenzone as evidenced by very low irritation potential.

KEY WORDS: *in vitro* erythemal UVA protection factor; *in vitro* SPF; irritation test; nanostructured lipid carriers (NLCs); oxybenzone; vitro-Skin™.

INTRODUCTION

Nowadays, the public awareness regarding the harmful effects of UV radiation combined with the problem of the ozone layer is increasing. Therefore, the use of sunscreens becomes necessary in daily life. There are two different ways of action for sunscreens: physical sunscreens and molecular sunscreens. Molecular sunscreens contain conjugated π-and n-electrons which are excited by certain wavelengths. The absorbed radiation is then re-emitted as lower energy rays, thus avoiding the skin harmful ultraviolet rays from reaching the skin (1). Oxybenzone is a widely used lipophilic, broad-spectrum molecular sunscreen agent, which effectively absorbs ultraviolet B (UVB) (290–320 nm), some ultraviolet A (UVA; 320–360 nm), and some ultraviolet C (250–290) (2). However, oxybenzone is the most common cause of photo-allergic contact dermatitis (3). In addition, systemic absorption of oxybenzone following its topical application to the skin has been reported (4).

Therefore, there is an urgent need for the development of safer sunscreen systems. This can be achieved by for-mulations that penetrate less into the skin or by formulations with a reduced amount of potentially dangerous molecular UV blocker while maintaining the sun protection factor by other means, e.g., carriers with sunblocking characteristics (5).

Nanostructured lipid carriers (NLCs) consisting of a lipid matrix with a special nanostructure had been developed as a new, improved generation of lipid nanoparticles (6). NLCs add additional benefits to the well-known opportunities of conventional solid lipid nanoparticles (SLNs) and are suited for topical use (7). In contrast to SLNs being produced from solid lipids, the NLCs are produced using blends of solid lipids (long chain) and liquid lipids (short chain) (8). Compared to SLNs, NLCs possess lower melting point due to their oil content, while maintaining their particulate character and being solid at body temperature (6).

Literature lacks any previous attempts to formulate oxybenzone as sole sun screening agent in nanostructured lipid carriers.

In the present study, we attempted to formulate oxybenzone-loaded NLCs. Then, a candidate formula with optimum physicochemical characterization was selected. This formula was then formulated into gel. Skin irritation test, *in vitro* sun protection factor (SPF), erythemal UVA protection factor of free oxybenzone and the candidate formula before and after formulation into gel were measured using Vitro- Skin™.

[1] Department of Pharmaceutics, National Organization of Drug Control and Research (NODCAR), Cairo, Egypt.

[2] Department of Pharmaceutics, Faculty of Pharmacy Cairo University, Kasr El Ainy street11562, Cairo, Egypt.

[3] To whom correspondence should be addressed. (e-mail: pharmnova @yahoo.com)

MATERIALS AND METHODS

Materials

Oxybenzone, was obtained from International Speciality Products, ISP, USA; Glyceryl monostearate (GMS) which is a mixture of 40–50% mono-, 30–45% di- and 5–15% triglycerides esters of stearic acid (C_{21}) and palmitic acid (C_{19}) with melting point of 55–66°C was obtained from Carl Roth GmbH, Germany; Miglyol 812 which is caprilic/capric triglycerides, was obtained from Goldschmidt GmbH, Germany; oleic acid was obtained from Riedel de-Haen, Germany; polyvinyl alcohol (PVA) of average molecular weight 146,000–186,000 was obtained from Celanese, USA; ethanol 95% and acetone were obtained from Riedel-de Haen GrambH, Germany; Carbopol 934 was obtained from Goodrich Chemical Co, USA. All other chemicals and solvents were of analytical grade.

Design of the Experiments

A complete 2^3 factorial design was used to study the effect of the liquid lipid type, liquid lipid concentration, and oxybenzone concentration on the particle size, the entrapment efficiency and the percentage of oxybenzone released after 8 h. Table I summarizes the independent variables along with their levels. The experimental results were analyzed using StatView Abacus Concept Version 4.57 software. The concentration of the total lipid (10%), type of solid lipid (glyceryl monostearate), concentration of PVA (1%) as well as solvent ratio 1:1 (ethanol/acetone (v/v)) were kept constant and were selected based on preformulation studies (data not shown).

Preparation of Oxybenzone Nanostructured Lipid Carriers

NLCs loaded with oxybenzone (5% or 10% w/w) were prepared by the solvent diffusion method in an aqueous system (9) with slight modification. The amount of the drug to be added (in grams) was calculated as a percentage of the lipid matrix as follows: 100 g of a 10% NLCs dispersion loaded with 5% drug contained 10 g solid consisting of 9.5 g lipid mixture (liquid lipid 1.425 g and GMS 8.075 g) and 0.5 g drug. For NLCs dispersion loaded with 10% drug, the proper amounts of the formulation ingredients were used.

The lipid mixture (GMS with Miglyol 812 or oleic acid) and oxybenzone were completely dissolved in a 12-ml mixture of ethanol and acetone 1:1 (v/v) in a water bath at 50°C. The resultant lipid solution was poured into 240 ml of an aqueous phase containing PVA (1% w/v) under mechan-

ical agitation using mechanical stirrer (Falc Instruments, Italy) at 400 rpm in a water bath at 70°C for 5 min. The obtained dispersion was allowed to cool to room temperature while stirring by a magnetic stirrer to get rid of organic solvents, and then oxybenzone-loaded NLCs were finally obtained.

Oxybenzone suspension (without adding lipids) and the placebo NLC dispersions (without adding the drug) were prepared exactly in the same manner. An overview of the composition of the NLCs is given in Table II.

Characterization of Oxybenzone Nanostructured Lipid Carriers

Transmission Electron Microscope

The morphology of the oxybenzone NLCs (selected samples were NLC4 and NLC8) was examined by the transmission electron microscope (JEM-100S, Jeol Ltd., Japan). Samples were prepared by the negative staining technique. The NLCs were dispersed directly into bidistilled water, and then copper grid coated with collodion film was put into the solution for several times. After being stained by 2% (w/v) phosphotungestic acid solution and dried at room temperature, the sample was ready for the transmission electron microscope (TEM) investigation at 70 kV (10).

Particle Size Analysis

Particle size and polydispersity index (PI) which is a measure of the distribution of nanoparticle population were determined by using laser scattering particle size distribution analyzer (LA-920, Horiba, Japan; detection limit 0.2–2,000 µm). One day after production, NLC dispersions were diluted with filtered bidistilled water, sonicated for 30 s, and subsequently analyzed. Three analyses were performed for each sample and the average values were taken. The obtained data were evaluated using the volume distribution ($d_{10\%}$, $d_{50\%}$, $d_{90\%}$) which means that if the diameter 90% ($d_{90\%}$) is registered as 1 µm, this indicates that 90% of particles have a diameter of 1 µm or lower. The PI was measured by the span which can be calculated from the following equation (11):

$$\text{Span} = \frac{d_{90\%} - d_{10\%}}{d_{50\%}}$$

Where $d_{90\%}$ is the particle diameter at 90% cumulative size, $d_{10\%}$ is the particle diameter at 10% cumulative size, and $d_{50\%}$ is the particle diameter at 50% cumulative size.

Table I. 2^3 Factorial Design for Preparation of Oxybenzone NLCs

Variables	Levels	
Liquid lipid type	Miglyol 812	Oleic acid
Liquid lipid conc. (% w/w)[a]	15	30
Oxybenzone conc. (% w/w)[b]	5	10

[a] Percent with respect to lipid mixture
[b] Percent with respect to lipid matrix

Table II. Composition of the Prepared Oxybenzone NLC Dispersions

Formulation code	Liquid lipid type	Liquid lipid conc. (% w/w)[a]	GMS[b] conc. (% w/w)[a]	Oxybenzone conc. (% w/w)[a]
NLC1	Miglyol 812	14.25	80.75	5
NLC2			75.75	10
NLC3		28.5	66.5	5
NLC4			61.5	10
NLC5	Oleic acid	14.25	80.75	5
NLC6			75.75	10
NLC7		28.5	66.5	5
NLC8			61.5	10

GMS glyceryl monostearate (the solid lipid used)
[a] Percent with respect to total lipid concentration which is 10% *w/w* of the formulation
[b] Concentration of PVA used is 1%

Zeta Potential (ζ)

The zeta potential was measured using the Zetasizer 2000 (Malvern Instruments Ltd., Malvern, UK). The solid lipid nanoparticle dispersions were diluted with 1 mM NaCl and placed in the electrophoretic cell where an electric field of 80 mV was established. Measurements were carried out in triplicate at 25°C. The electrophoretic mobility and hence zeta potential was calculated directly from the apparatus using the Smolochowski equation (12)

Determination of Oxybenzone Entrapment Efficiency Percent

The drug-loaded NLC dispersion was uniformly mixed by gentle shaking; 1.0 ml of this dispersion was diluted with 9.0 ml methanol, centrifuged by using High-Speed Refrigerated Centrifuge (3K30, SIGMA, Germany) for 45 min at 16,000 rpm and then filtered using Millipore® membrane (0.2 μm). The filtrate was collected and appropriately diluted with methanol and measured spectrophotometrically (Shimadzu, model UV-2450, Kyoto, Japan) at λ_{max} of 286 nm (13). The entrapment efficiency percent (EE%) was calculated using the following equation (9):

$$\text{Entrapment efficiency} (EE\,\%) = \frac{Wa - Ws}{Wa} \times 100$$

Where Wa and Ws were the weight of drug added in system and the analyzed weight of drug in supernatant, respectively.

In vitro Release Studies of Oxybenzone from NLCs: Franz Diffusion Cells

For this investigation, static Franz glass diffusion cells (Microette plus, Hanson Research, USA) were used (14). These cells consist of donor and receptor chambers between which a cellulose membrane (MEMBRA-CEL dialysis tubing with molecular weight cutoff 3,500–7,000 Da, Serva Electrophoresis GmbH, Germany) was positioned; area of diffusion was 1.7 cm². The dialysis membrane was hydrated in receptor medium [methanolic buffer solution (phosphate-buffered saline pH 7.4/methanol (3:2) (*v/v*))] for 12 h before mounting into the Franz diffusion cell. Oxybenzone NLC dispersion (2 mg/cm²) was placed in the donor chamber and the receptor chamber was filled with 7.5 ml receptor medium and stirred continuously at 100 rpm at 37°C in order to ensure the surface skin temperature of 32°C on the surface of the membrane (14). After 1, 2, 3, 4, 5, 6, 7, and 8 h, 2 ml were withdrawn from the receptor chamber through a side-arm tube. After each withdrawal of sample, an equal volume of receptor medium was added in the receptor chamber so as to maintain a constant volume throughout the study. Samples were analyzed for oxybenzone concentration using ultraviolet spectrophotometry at 289.4 nm.

Effect of Storage Temperature on Particle Size and Entrapment Efficiency of the Prepared NLCs

Oxybenzone NLC dispersions were divided into two sample sets of capped vials protected from light, one stored in a refrigerator at 2–8°C and the other stored at room temperature (25°C). Samples were withdrawn after 3 months and subjected to particle size and entrapment efficiency measurements.

Formulation of NLC-Based Hydrogel

Based on the previously mentioned characterization, and the results of the main effects of the adopted factorial design a candidate formula NLC4 (containing 1% oxybenzone) with optimum physicochemical properties was selected. The selected NLC4 dispersion was formulated into hydrogel (NLC4G) by adding 1% (*w/w*) Carbopol 934 under magnetic stirring at 800 rpm. Stirring was continued until carbopol is dispersed. The dispersions were neutralized using triethanolamine solution (15). Hydrogel formulations containing either 1% oxybenzone suspension (1% oxy G) and placebo NLC4 (pNLC4G) were prepared for comparison.

Characterization of the Prepared Gels

Rheological Studies

The viscosity and rheological behavior of the gel formulations were determined using a cone and plate viscometer (Brookfield Engineering Laboratories, model HADV-II, Middleboro, MA, USA). All measurements were carried out at a temperature of 25°C±1, using spindle CP52. The shear rate in s^{-1}, the shear stress in dyne/cm² and the viscosity in centipoise were determined. The rheological parameters of different gels were studied (16).

Skin Irritation Test

The study protocol and subject informed consent were approved by the institutional review board of Faculty of Pharmacy, Cairo University (IRB00007140) and the study was conducted according to the Declaration of Helsinki (17) and the International Conference on Harmonization of Technical requirements for Registration of Pharmaceutics for Human Use Guidance for good clinical practice (18).

Ten healthy subjects (aged from 23 to 40 years) were participated in this study. The participants were briefed on the study procedures and a written informed consent was obtained from all subjects prior to conducting procedure.

Each formulation (pNLC4, NLC4, and 1%oxybenzone suspension) and their corresponding hydrogels (pNLC4G, NLC4G and 1% oxy G) was applied once to each volunteer, at a dose of 0.3 g on a surface area of 5 cm^2 on forearm. After 6 h, the test specimen was thereafter washed off by tap water and observed for any visible change such as erythema (redness). The mean erythemal scores were recorded (ranging from 0 to 4) according to Draize scale (19). Where, 0 means no erythema, 1 slight erythema, 2 moderate erythema, 3 moderate to severe erythema, and 4 severe erythema.

In vitro UV Blocking Ability

The Transpore® assay (20) is an *in vitro* method to investigate the UV blocking ability of the investigated dispersions (pNLC4, NLC4, and 1%oxybenzone suspension). A concentration of 2 mg/cm^2 of the formulation was spread evenly on top of the Transpore tape® (3M Australia Pty Ltd., Australia) which was placed on a quartz cuvette. After a drying period of 15 min, the samples were scanned spectrophotometrically from 250 to 400 nm and the absorption was measured.

In vitro SPF and Erythemal UVA Protection Factor Measurement

The SPF mainly represents the protection against UVB (21). For this reason, the new developments in sunscreens have to provide a description of the protection against not only the UVB radiation, but also the UVA one (22). The determination of the SPF of the formulations was conducted according to the method described by Diffey and Robson (23). Vitro-Skin™, a registered trademark of IMS, is an advanced testing substrate used for *in vitro* measurement of SPF. It contains both optimized protein and lipid components and is designed to have topography, pH, critical surface tension, and ionic strength similar to human skin. It is the substrate that gives the most consistent correlation with published *in vivo* SPF measurements (24). It was used for sample application. It was hydrated by placing it on the shelf of a closed, controlled-humidity chamber (containing 85% water/15%glycerin in its bottom) for 16–24 h prior to its use (25) and then placed on a quartz cuvette. The intensity of radiation transmitted through the substrate was determined automatically by recording the photocurrent in 5-nm steps from 290 to 400 nm. An appropriate weight (2 mg/cm^2) of each formulation (pNLC4, NLC4, and 1% oxybenzone

suspension) and their corresponding hydogels (pNLC4G, NLC4G and 1% oxyG) was applied to the substrate surface by spotting it at several sites over the application area (4.5 cm^2). After a drying period of 15 min, transmission measurements were done. These experiments were run in triplicates

The *in vitro* SPF can be calculated according to the following equation (23):

$$\text{SPF} = \sum_{290}^{400} E_\lambda B_\lambda \Big/ \sum_{290}^{400} \left(E_\lambda B_\lambda / \overline{\text{MPF}_\lambda} \right),$$

Where E_λ, spectral irradiance of terrestrial sun light under defined conditions; B_λ, erythemal effectiveness; MPF_λ, the monochromatic protection factor at each wavelength increment which is measured as the ratio of the detector signal intensity without sunscreen applied to the substrate, to that with sunscreen applied to the substrate.

Considering the UVA wavelength range (320–400 nm) and using the terms of SPF equation, the *in vitro* erythemal UVA protection factor could be calculated according to the following equation (26).

$$\text{Erythemal UV} - \text{A protection factor} = \sum_{320}^{400} E_\lambda B_\lambda \Big/ \sum_{320}^{400} \left(E_\lambda B_\lambda / \overline{\text{MPF}_\lambda} \right).$$

RESULTS AND DISCUSSION

In this study, 10% GMS (as solid lipid), Miglyol and oleic acid (as liquid lipids), and 1% PVA (as stabilizer) were used to produce NLCs in order to enhance the sun screening efficacy and safety of the chemical sunscreen oxybenzone.

NLCs were produced using the solvent diffusion method. This technique offers advantages over existing methods such as the use of pharmaceutically acceptable organic solvents, easy handling, and a fast production process (27).

Characterization of the Prepared NLCs

Transmission Electron Microscope

Figure 1 shows the transmission electron micrographs of oxybenzone NLCs prepared using Miglyol 812 (NLC4) or oleic acid (NLC8) as liquid lipids. Both micrographs showed spherical but not perfectly round-shaped particles that did not stick to each other.

Regarding the size, both Miglyol 812 and oleic acid NLCs had small particle size ranged from 10 to 40 nm and from 40 to 60 nm, respectively. However, in order to obtain more precise information on particle size, laser scattering was used.

Particle Size Analysis

Mean particle size, particle size distribution ($d_{10\%}$, $d_{50\%}$, and $d_{90\%}$) and polydispersity index (P.I.) of different NLCs are depicted in Table III. All oxybenzone NLCs showed a considerable small particle size with $d_{90\%}$ less than 1 μm and with P.I. ranging from 0.454 to 0.597 and from 0.528 to 0.641 for oleic acid and Miglyol 812 NLCs, respectively.

The diameters determined by laser scattering were considerably larger when compared to the results obtained
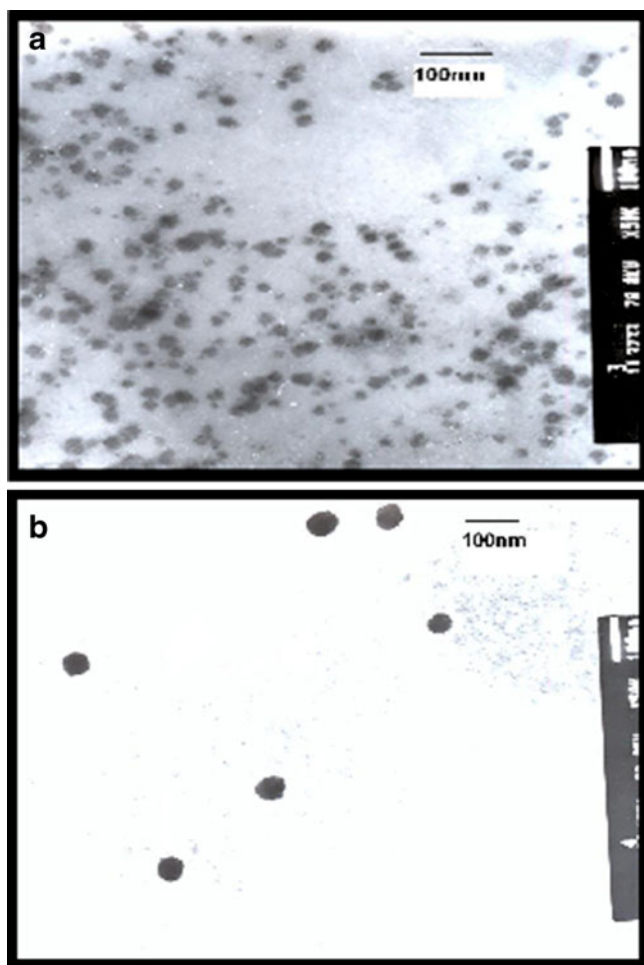
Fig. 1. Transmission electron microscope photograph of oxybenzone nanostructured lipid carriers using: **a** Miglyol (NLC4), **b** oleic acid (NLC8)

from TEM. This might be due to that the two methods are based on totally different mechanisms and employing different sample preparation processes, which might lead to the discrepancy of the outcomes. The size detection of NLCs by laser scattering was carried out in aqueous state and in this case, lipid nanoparticles were well hydrated and the diameters were 'hydrated diameters', which were usually bigger than their real diameters. In the case of TEM sample

preparation, all the free water and even some of hydrated water was stained. This implies that the sizes of NLCs derived from TEM might be considerably smaller than their real diameters (28).

Concerning the liquid lipid type, oleic acid significantly ($p<0.0001$) increased the particle size when compared to Miglyol 812. This may be due to the higher viscosity of oleic acid at 20°C (36.56 cps) (29) when compared to that of Miglyol 812 (28–32 cps) (30) at the same temperature. Consequently, this could be considered as the most important factor for the larger size of oleic acid NLCs. Hence, the mean particle size of lipid nanoparticles usually increased with increasing viscosity of the oil phase (31).

Concerning the two concentrations of both liquid lipids (Miglyol 812 and oleic acid) used, 30% gave significantly ($p<0.0001$) smaller particle size when compared to that of 15%. This could be attributed to that the higher liquid lipid content which reduced the viscosity inside NLCs, and consequently, reduced the surface tension to form smaller and smoother surface particles (32).

Increasing the oxybenzone concentration led to significant ($p<0.0001$) increase in particle size. This could be due to the higher melting point of oxybenzone (66–68°C) (33) when compared to that of GMS (the solid lipid used; 54–66°C) (30) which resulted in a more viscous dispersed phase, making difficult the mutual dispersion of the phases and originating larger particles (34). Similarly, Deli *et al.* (35) observed that the volume average diameter of NLCs increased as the amounts of drug increased.

Entrapment Efficiency

The entrapment efficiency of oxybenzone within the different prepared nanostructured lipid carrier formulations is shown in Table III. High entrapment efficiency of oxybenzone in all the prepared NLCs was observed, and was found to vary from 74.9%±3.0 for NLC6 using 15% oleic acid and 10% oxybenzone to 93.7%±3.2 for NLC4 using 30% Miglyol 812 and 10% oxybenzone (with respect to total lipid concentration).

Concerning liquid lipid type, Miglyol 812 significantly ($p<0.0001$) increased the entrapment efficiency when compared to oleic acid. Miglyol 812, being mixture of triglycerides of different chain length (C_8, C_{10}) (36) form less perfect crystals with many imperfections offering space to accommodate the drug

Table III. Particle Size Distribution, Mean Particle Size, Polydispersity Index (P.I) Entrapment Efficiency (E.E %), and Zeta Potential Values of Different Nanostructured Lipid Carriers

Formulation code	Mean volume distribution (μm±SD)			Mean particle size (μm ± SD)	P.I.	EE%±SD	Zeta potential±SD
	$d_{10\%}$	$d_{50\%}$	$d_{90\%}$				
NLC1	0.201	0.304	0.402	0.327±0.03	0.594	78.8±2.6	−14.00±0.5
NLC2	0.235	0.407	0.743	0.461±0.03	0.528	79.2±1.9	−13.90±1.0
NLC3	0.154	0.208	0.282	0.213±0.05	0.641	85.2±1.3	−21.03±1.2
NLC4	0.195	0.313	0.593	0.366±0.09	0.558	93.7±3.2	−19.30±0.6
NLC5	0.411	0.670	1.103	0.725±0.08	0.583	77.9±2.4	−29.70±1.8
NLC6	0.360	0.708	1.339	0.797±0.10	0.479	74.9±3.0	−18.80±0.8
NLC7	0.155	0.225	0.652	0.413±0.06	0.597	82.6±1.4	−16.70±0.5
NLC8	0.204	0.405	0.941	0.501±0.02	0.454	80.2±1.5	−10.60±0.3

(37) when compared to oleic acid which is a monounsaturated fatty acid form of stearic acid (38).

For liquid lipid concentration, 30% was found to significantly ($p<0.0001$) increase the entrapment efficiency when compared to 15%. This could be attributed to the fact that drug solubility is greater in liquid lipids than in solid lipids. Increasing liquid lipid content into the solid lipid matrix (GMS) could increase the solubility of the drug in the lipid matrix, which increased its entrapment efficiency (8). Furthermore, it was reported (39) that the incorporation of liquid lipid to solid lipid could led to great imperfections in the crystal lattice and left enough space to accommodate drug molecules, thus leading to improved drug entrapment efficiency.

Regarding oxybenzone concentration, 10% *w/w* (based on total lipid concentration) was found to have a non-significant effect ($p>0.05$) on entrapment efficiency when compared to 5% *w/w*.

Effect of Storage Time and Temperature on Particle Size and Entrapment Efficiency of the Prepared NLCs

The physical stability of Miglyol 812 and oleic acid NLCs formulations was suggested by the absence of visible phase separation and all dispersions remained in a homogeneous state upon storage at 2–8°C and room temperature (25°C) for 90 days. The mean particle size of the prepared NLCs after storage at both temperatures is shown in Fig. 2. Non-significant increase was observed in the particle size for the samples stored at 2–8°C over the monitored period while those stored at room temperature showed slight increase in the mean particle size but they remained less than 1.0 μm. This was in agreement with Sharma *et al.* (38) and Junyaprasert *et al.* (40) who observed that there was no significant increase in particle size of NLCs when stored for 3 months at different temperatures.

Figure 3 shows the relationship between entrapment efficiency and storage temperatures of NLCs. It was observed that NLCs exhibited a good ability to reduce the drug expulsion during storage at refrigerated (2–8°C) and room temperature. This could be attributed to the incorporation of

liquid lipid to solid lipid matrix, which increased the imperfection in crystal order of matrix and reduced the crystallization process on storage, and thus prevent drug expulsion (6).

In vitro Release Study: Franz Diffusion Cells

The *in vitro* release profile of oxybenzone from the nanostructured lipid carriers was investigated over 8 h. The results are shown in Fig. 4a and b.

Concerning liquid lipid type, Miglyol 812 NLCs produced significantly ($p<0.05$) slower *in vitro* release after 8 h when compared to oleic acid NLCs. This might be due the homogeneous entrapment of oxybenzone throughout the systems when using Miglyol 812. It was previously stated (10) that the slow release of the drug from lipid nanoparticles suggests homogeneous entrapment of the drug throughout the systems. Consequently, Miglyol 812NLCs with higher entrapment efficiency when compared to oleic acid NLCs showed slower release profiles.

Concerning liquid lipid concentration, the extent of drug released was significantly higher ($p<0.0001$) upon using 30% when compared to 15%. This could be attributed to the smaller particle size of the prepared NLCs with higher liquid lipid content. Similar increase in release was observed by Jenning *et al.* (7) and Teeranachaideekul *et al.* (31). It was previously stated (41) that for small particles, particularly in the nanometer size, the saturation solubility would significantly increase. Both the increase in the saturation solubility and the enlargement of the surface area contribute to the enhancement of dissolution velocity and consequently faster release rate would therefore be expected. It was also observed from Fig. 4a and b that NLCs loaded with higher oxybenzone concentration showed significantly slower ($p<0.0001$) release profile when compared to lower concentrations. This could be attributed to that higher drug concentration decreases the diffusion rate through the carrier. This is due to the incorporation model. Higher drug concentration led to the formation of drug-enriched core model (the drug occupies the core of the particles) which promote slower release (14,42).
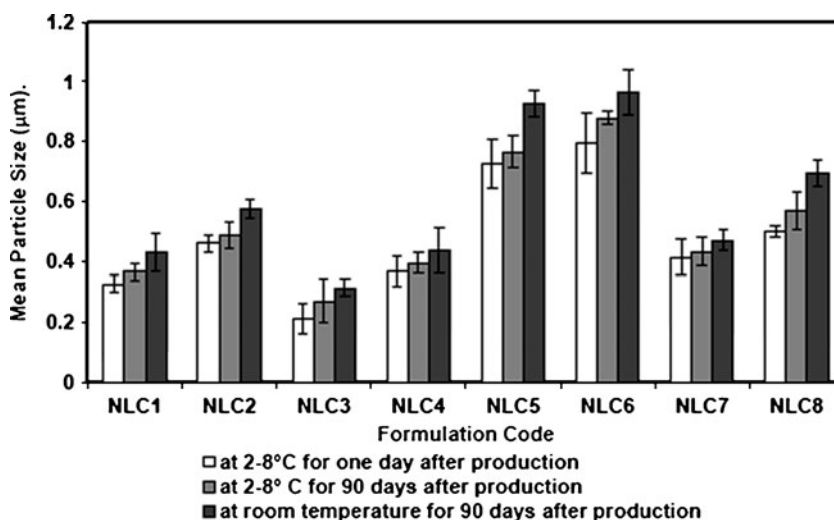

Fig. 2. Effect of storage temperature on the mean particle size of oxybenzone NLC formulations
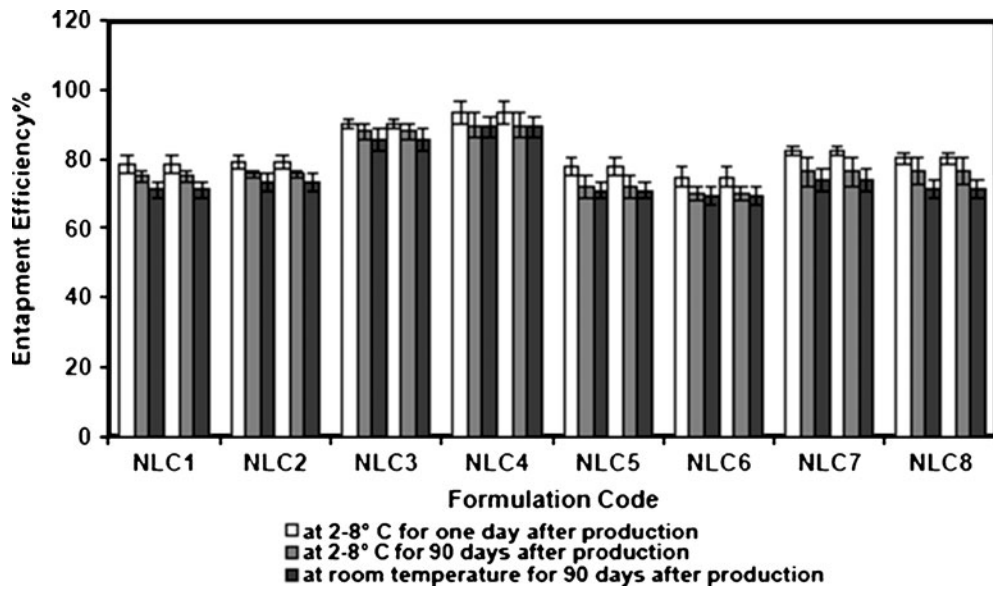
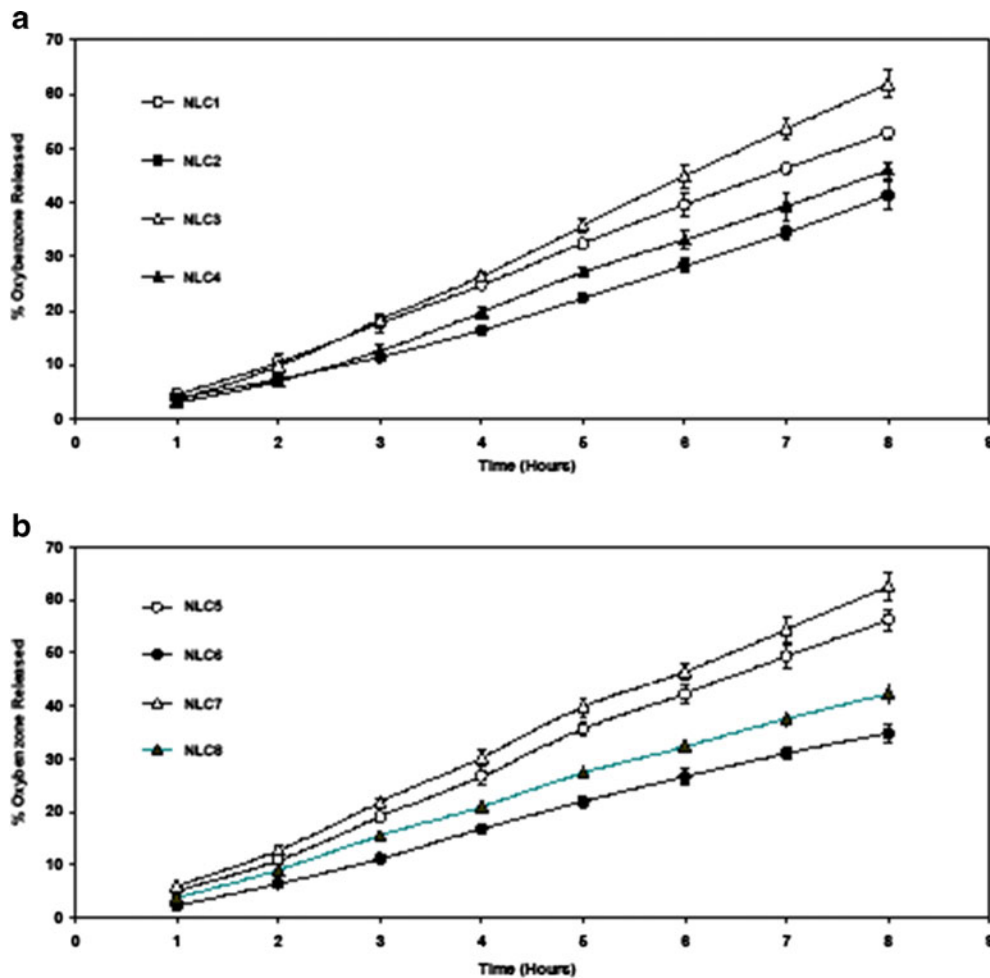**Fig. 3.** Effect of storage temperature on the entrapment efficiency of oxybenzone NLC formulations

Fig. 4. Release profile of oxybenzone from NLC formulations prepared using different liquid lipids and oxybenzone concentrations **a** miglyol, **b** oleic acid

Zeta Potential (ζ)

Zeta potential was measured to evaluate the stability of NLC dispersions (Table III). All NLCs were negatively charged. The negative charge was likely caused by the slightly ionized fatty acids from glycerides including the negatively charged miglyol 812 and oleic acid at their carboxylic groups (43). Values of zeta potential ranged from -10.6 ± 0.3 mV for NLC8 using 30% oleic acid and 10% oxybenzone to -29.7 ± 1.8 mV for NLC5 using 15% oleic acid and 5% oxybenzone. Generally, zeta potential values of all NLCs in this study were above |8–9|mV, which was a prerequisite for the stability of the nanoparticles, prepared using a steric stabilizer (PVA) (44).

Concerning the effect of drug concentration on zeta potential, it was noticed that the absolute values of zeta potential decreased as the amounts of drug added increased. The larger particle size obtained upon increasing the drug concentration led to the lower charge density of particle and absolute values of zeta potential (45). No linear correlation between the zeta potential and liquid lipid concentration of NLCs on the zeta potential was observed. This was in agreement with Chen *et al.* (46) who observed that different squalene (liquid lipid) ratios did not affect zeta potential of the prepared NLCs.

Based on the previous characterization and analysis of the main effects of the independent variables of the adopted factorial design NLC4 dispersion (see Table II for composition) showed the highest EE% (93.7%±3.2), adequate zeta potential (−19.30 mV±0.6), slow drug release (46.05% after 8 h), and adequate small particle size (0.366 µm±0.09), was chosen as candidate NLC dispersion which was then formulated into gel and its rheological properties, skin irritation, UV blocking ability, SPF, and its UVA-PF were studied and compared with that of placebo NLC4 and 1% oxybenzone suspension.

Characterization of the Prepared Gels

Rheological Studies

Due to the low viscosity of NLC dispersions, it could be assumed that they were not suitable as topical or dermal delivery systems. To cope with this problem, one possibility would be incorporation into hydrogels or creams (40).

Carbopol 934 gel and the liquid lipid Miglyol 812 were selected for the preparation of NLCs because of their excellent skin properties. Carbopol, is used due its compatibility with nanoparticulate dispersions, ease of preparation, esthetic appeal, thermal stability and optimum rheological properties while Miglyol 812 (a mixture of triglycerides), is chosen because the lipid composition of the epidermis is mainly based on triglycerides (25%) (47).The freshly prepared gel bases were subjected to determination for their rheological characteristics at 25°±1C. Rheograms are shown in Fig. 5. The results revealed that all gel formulations exhibited pseudoplastic flow characteristics with thixotropy. NLC4 gel formulations either placebo or oxybenzone loaded had higher thixotropy than that of 1% oxybenzone gel. Additionally, it was observed that placebo and oxybenzone loaded NLC4 possessed higher viscosity when compared to
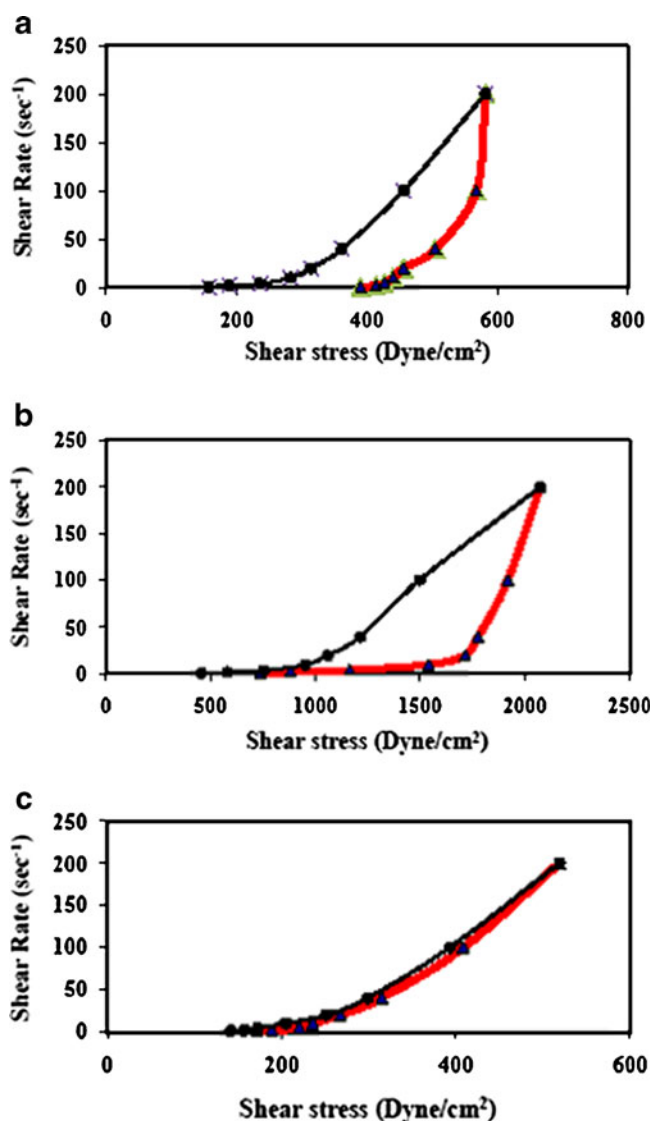

Fig. 5. Rheograms of **a** placebo NLC4 gel, **b** NLC4 gel, and **c** 1% oxybenzone gel measured at a temperature of 25°±1C

that of 1% oxybenzone gel (data not shown). This was due to the presence of solid lipid (GMS) constituting the NLC4 which acted as consistency imparting agent (16).

Skin Irritation Test

Results of skin irritation test are shown in Table IV. No irritation or erythema was observed for placebo NLC4 either in dispersion or in gel forms, mean score±SD=0 and only very slight erythema of (0.2±0.4) was observed for oxybenzone-loaded NLC4 dispersion and the corresponding gel. Conversely, 1% oxybenzone suspension and its corresponding gel showed a well-defined erythema of 1.5±0.5. This could be attributed to the high entrapment efficiency of oxybenzone in NLC4 (93.7%±3.2) which might be beneficial to reduce the skin irritation of drug due to avoidance of the direct contact between drug and skin surface (48). This was in agreement with Joshi *et al.* (49) who observed that NLC-based gel of Valdecoxib showed no skin irritation compared with the

Table IV. Skin Irritation Test of Placebo NLC4, Oxybenzone-Loaded NLC4 and 1% Oxybenzone Dispersions and Their Corresponding Gels

Formulation code	Reaction in volunteers (mean±SD)
	$N=10$
pNLC4	0±0.00
NLC4	0.2±0.42
1%Oxy.	1.5±0.537
pNLC4G	0±0.00
NLC4G	0.2±0.42
1%Oxy.G	1.4±0.52

Fig. 7. SPF values of different oxybenzone-loaded NLCs formulations and oxybenzone suspension using vitro skin as substrate

marketed formulation containing the drug in the free form, which showed irritation upon application.

In vitro UV Blocking Ability

The wavelength scans of the placebo NLC4 (p NLC4), oxybenzone-loaded NLC4 (NLC4) and 1% oxybenzone suspension (1% oxy) are given in Fig. 6 It was observed that the absorbance caused by placebo NLC4 was slightly higher than that caused by 1% oxybenzone suspension. This was attributed to that nanoparticles were considered as scatterers/reflectors of UV radiation (5).
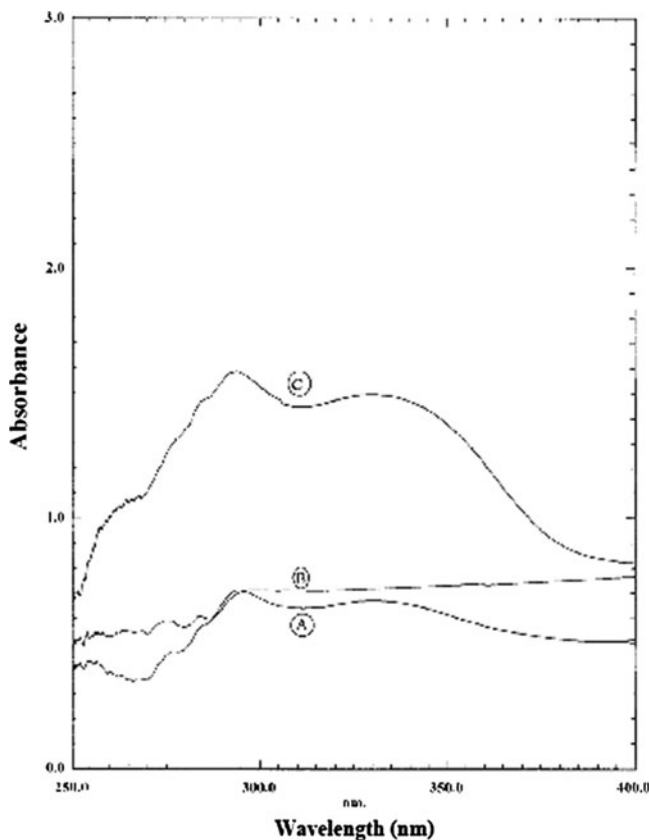
It was also observed that the absorption spectrum of oxybenzone-loaded NLC4 was shifted to higher values by about threefold when compared to 1% oxybenzone suspension. This was in accordance with Xia *et al.* (50) who observed that the sunscreen-loaded NLC gave higher absorbance when compared to that of reference emulsion with the same sunscreen content. This might be attributed to the synergistic photoprotection caused by the incorporation of sunscreens into a nanoparticle formulation (51).

It must be mentioned that NLC4 was the candidate NLC although it did not possess the smallest particle size; this was because its mean particle size (0.366 µm±0.09) was adequate for UV blocking effect. It was stated that there was an optimal size for the maximum UV absorption (about 375 nm mean particle size). This could be explained as follows, when the particles became smaller the surface/volume ratio become higher, i.e., there are more surfaces where the light is reflected, absorbed, or refracted. But when the particles were smaller than a definite particular size (smaller that 370 nm) they become transparent, and hence the absorption of UV radiation decreases. Moreover, for particles of smaller size, the destructive interference of the particles with the radiation beam becomes very small, i.e., these very small particles do not absorb, refract, or reflect the light as the relatively bigger ones (52).

In vitro SPF and EUVA-PF

The results of SPF and EUVA-PF of the investigated formulations are depicted in Figs. 7 and 8. The results revealed that there was no pronounced difference between SPF values obtained by placebo NLC4 (5.10±0.36) and 1%

Fig. 6. Wavelength scans of 1% oxybenzone suspension (1%oxy), **a** placebo NLC 4 dispersion (PNLC4), **b** and 1% oxybenzone-loaded NLC dispersion (NLC4), and (**c**) obtained by the Transpore® tape assay
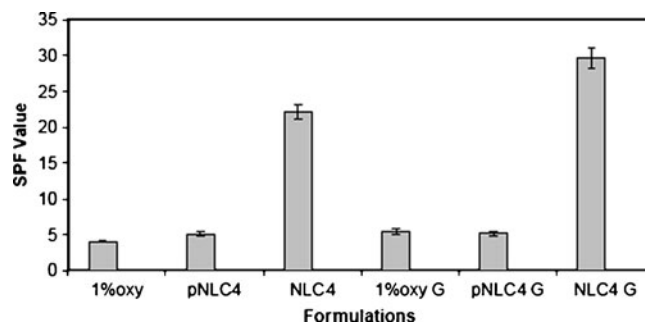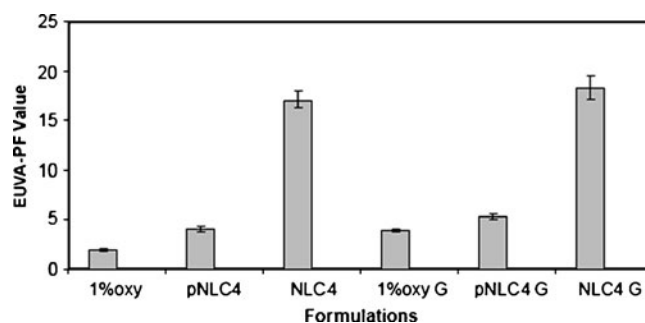

Fig. 8. Erythemal UVA protection factor of different oxybenzone loaded NLCs formulations and oxybenzone suspension using vitro skin as substrate

oxybenzone suspension (4.07±0.13). However, oxybenzone-loaded NLC4 dispersion gave higher SPFs 22.20±1.00 which is about sixfold higher than that of 1% oxybenzone suspension. In case of 1% oxybenzone suspension, it had low EUVA-PF, of about 1.90±0.20. Conversely, in the case of oxybenzone-loaded NLC4, high EUVA-PFs of 17.10±0.85 which corresponded to about eightfold increase in EUVA-PFs was observed.

The obtained SPFs and EUVA-PFs demonstrated the advantages of the use of mixed particles composed of liquid and solid lipids (NLCs) as carrier system for UV filters. Although oxybenzone was directly responsible for the UV absorption in those carriers, the use of Miglyol 812 was justified in virtue of its low viscosity enabling a good distribution of oxybenzone inside the GMS matrix. Similarly, Hernandez *et al*. (53) used the oil 'decyl oleate' to ensure a good distribution of sunscreen into the solid matrix of NLC to enhance its sun protection efficacy.

The SPF and EUVA-PF results also revealed that all gel formulations showed better sun protection factor compared to their corresponding dispersions where the SPF values of NLC4 gel reached 29.6±1.40 and the EUVA-PF reached 18.3 ±1.20 compared to 22.20±1.00 and 17.10±0.85 in case of the dispersions, respectively . Anderson *et al*. (54) demonstrated that the increase in the viscosity of the cosmetic preparations was directly related to an increased SPF. This could be partially attributed to an increase in viscosity providing the pigments with a better fixation on the plates during the SPF measurements.

CONCLUSION

The present work has shown that NLCs containing lipophilic sunscreen oxybenzone can be produced by the solvent diffusion method. The advantage of this method is the instantaneous and reproducible formation of NLCs exhibiting a high degree of entrapment efficiency. Formulation of oxybenzone into NLCs enhanced the efficiency of sunscreens formulation. The encapsulation of sunscreen agent in NLCs also provided the advantage of overcoming solubility and skin irritancy problems. Oxybenzone is insoluble in water and is difficult to incorporate in a gel base. After entrapment of oxybenzone in NLCs, it could be easily incorporated into gel base without any crystallization problem common with oxybenzone. The topical application of gel formulation containing NLCs of oxybenzone may be more efficient in protecting against UVA and UVB radiation; probably due to the film formation over the skin, which itself acts as a physical barrier to UV radiations. In conclusion, the results of this study emphasize the potential of NLCs using Miglyol 812 and glyceryl monostearate as a new topical drug delivery system for enhancing the sunscreening efficacy of oxybenzone by about sixfold while reducing its side effects

ACKNOWLEDGMENTS

REFERENCES

1. Rai R, Srinivas CR. Photoprotection. Indian J Dermatol Venereol Leprol. 2007;73:73–9.
2. Patel M, Jain SK, Yadav AK, Gogna D, Agrawal GP. Preparation and characterization of oxybenzone-loaded gelatin microspheres for enhancement of sunscreening efficacy. Drug Deliv. 2006;13:323–30.
3. Cook N, Freeman S. Report of 19 cases of photoallergic contact dermatitis to sunscreens seen at the skin and cancer foundation. Australas J Dermatol. 2001;42:257–9.
4. Benson HAE, Sarveiya V, Risk S, Roberts MS. Influence of anatomical site and topical formulation on skin penetration of sunscreens. Ther Clin Risk Manag. 2005;1:209–18.
5. Wissing SA, Muller RH. The development of an improved carrier system for sunscreen formulations based on crystalline lipid nanoparticles. Int J Pharm. 2002;242:373–5.
6. Pardeike J, Hommoss A, Muller RH. Lipid nanoparticles (SLN, NLC) in cosmetic and pharmaceutical dermal products. Int J Pharm. 2009;366:170–84.
7. Jenning V, Thunemann AF, Gohla SA. Characterisation of a novel solid lipid nanoparticle carrier system based on binary mixtures of liquid and solid lipids. Int J Pharm. 2000;199:167–77.
8. Muller RH, Radtke M, Wissing SA. Nanostructured lipid matrices for improved microencapsulation of drugs. Int J Pharm. 2002;242:121–8.
9. Hu FQ, Jiang SP, Du YZ, Yuan H, Ye YQ, Zeng S. Preparation and characteristics of monostearin nanostructured lipid carriers. Int J Pharm. 2006;314:83–9.
10. Paliwal R, Rai S, Vaidya B, Khatri K, Goyal AK, Mishra N, *et al*. Effect of lipid core material on characteristics of solid lipid nanoparticles designed for oral lymphatic delivery. Nanomedicine. 2009;5:184–91.
11. Chew NYK, Chan HK. Effect of powder polydispersity on aerosol generation. J Pharm Pharm Sci. 2002;5:162–8.
12. Teeranachaideekul V, Souto EB, Muller RH, Junyaprasert VB. Physicochemical characterization and *in vitro* release studies of ascorbyl palmitate-loaded semi-solid nanostructured lipid carriers (NLC gels). J Microencapsul. 2008;25:111–20.
13. The United States Pharmacopeia, (USP30) & national formulary National Formulary NF the official compendia of standards. Michigan: United States Pharmacopeial Convention, Inc; 2007. pp. 2820
14. Wissing SA, Muller RH. Solid lipid nanoparticles as carrier for sunscreens: *in vitro* release and *in vivo* skin penetration. J Control Release. 2002;81:225–33.
15. Shah KA, Date AA, Joshi MD, Patravale VB. Solid lipid nanoparticles (SLN) of tretinoin: potential in topical delivery. Int J Pharm. 2007;345:163–71.
16. Gaspar LR, Maia Campos PMBG. Rheological behavior and the SPF of sunscreens. Int J Pharm. 2003;250:35–44.
17. Declaration of Helsinki–Current (2008) version Available at http://www.wma.net/e/policy/pdf/17c.pdf
18. Guidelines for Good Clinical Practice. European Medicines Agency, CPMP/ICH/135/95 July2002
19. Campbell RL, Bruce RD. Direct comparison of rabbit and human primary skin irritation responses to isopropylmyristate. Toxicol Appl Pharmacol. 1981;59:555–63.
20. Wissing SA, Muller RH. Solid lipid nanoparticles (SLN)—a novel carrier for UV blockers. Pharmazie. 2001;56:783–6.
21. Bernerd F, Vioux C, Lejeune F, Asselineau D. The sun protection factor (SPF) innadequately defines broad spectrum photoprotection:demonstration using skin reconstructed *in vitro* exposed to UVA, UVB or UV-solar simulated radiation. Eur J Dermatol. 2003;13:242–9.
22. Moyal D, Chardon A, Kollias N. Determination of UVA protection factors using the persistent pigment darkening (PPD) as the end point (part 1) calibration of the method. Photodermatol Photoimmunol Photomed. 2000;16:245–9.
23. Diffey BL, Robson J. A new substrate to measure sunscreen protection factors throughout the ultraviolet spectrum. J Soc Cosmet Chem. 1989;40:127–33.

24. Springsteen A, Yurek R, Frazier M, Carr KF. *In vitro* measurement of sun protection factor of sunscreens by diffuse transmittance. Anal Chim Acta. 1999;380:155–64.

25. Vitro Skin™. 2009. http://www.ims-usa.com

26. Villalobos-Hernandez JR, Muller-Goymann CC. Novel nanoparticulate carrier system based on carnauba wax and decyl oleate for the dispersion of inorganic sunscreens in aqueous media. Eur J Pharm Biopharm. 2005;60:113–22.

27. Zhang J, Fan Y, Smith E. Experimental design for the optimization of lipid nanoparticles. J Pharm Sci. 2009;98:1813–9.

28. Liu J, Gong T, Wang C, Zhong Z, Zhang Z. Solid lipid nanoparticles loaded with insulin by sodium cholate-phosphatidylcholine-based mixed micelles: preparation and characterization. Int J Pharm. 2007;340:153–62.

29. Viscosity of liquids: theory, estimation, experiment, and data. Viswanath DS, Ghosh TK, Prasad DHL, Dutt NVK, Rani KY, editors. Springer, Dordreecht; 2007 pp. 295

30. Handbook of pharmaceutical excipients 5th ed. Rowe RC, Sheskey PJ, Owen SC, editors. London: Pharmaceutical Press; 2006. pp. 454, 308

31. Teeranachaideekul V, Boonme P, Souto EB, Muller RH, Junyaprasert VB. Influence of oil content on physicochemical properties and skin distribution of Nile red-loaded NLC. J Control Release. 2008;128:134–41.

32. Hu FQ, Jiang SP, Du YZ, Yuan H, Ye YQ, Zeng S. Preparation and characterization of stearic acid nanostructured lipid carriers by solvent diffusion method in an aqueous system. Colloids Surf B Biointerfaces. 2005;45:167–73.

33. Felton LA, Wiley CJ, Godwin DA. Influence of hydroxypropyl β-cyclodextrin on the transdermal permeation and skin accumulation of oxybenzone. Drug Dev Ind Pharm. 2002;28:1117–24.

34. Mainardes RM, Evangelista RC. PLGA nanoparticles containing praziquantel: effect of formulation variables on size distribution. Int J Pharm. 2005;290:137–44.

35. Deli G, Hatziantoniou S, Nikas Y, Demetzos C. Solid lipid nanoparticles and nanoemulsions containing ceramides: preparation and physicochemical characterization. J Liposome Res. 2009;19:180–8.

36. Nankervis R, Davis SS, Day NH, Shaw PN. Effect of lipid vehicle on the intestinal lymphatic transport of isotretinoin in the rat. Int J Pharm. 1995;199:173–81.

37. Li F, Wang Y, Liu Z, Lin X, He H, Tang X. Formulation and characterization of bufadienolides-loaded nanostructured lipid carriers. Drug Dev Ind Pharm. 2010;36:508–17.

38. Sharma P, Ganta S, Denny WA, Garg S. Formulation and pharmacokinetics of lipid nanoparticles of a chemically sensitive nitrogen mustard derivative: chlorambucil. Int J Pharm. 2009;367:187–94.

39. Ali H, El-Sayed K, Sylvester PW, Nazzal S. Molecular interaction and localization of tocotrienol-rich fraction (TRF) within the matrices of lipid nanoparticles: evidence studies by Differential Scanning Calorimetry (DSC) and proton nuclear magnetic resonance spectroscopy (^{1}H NMR). Colloids Surf B Biointerfaces. 2010;77:286–97.

40. Junyapraserta VB, Teeranachaideekul V, Souto EB, Boonme P, Muller RH. Q10-loaded NLC *versus* nanoemulsions: stability, rheology and *in vitro* skin permeation. Int J Pharm. 2009;377:207–14.

41. Hou DZ, Xie CS, Huang KJ, Zhu CH. The production and characteristics of solid lipid nanoparticles (SLNs). Biomaterials. 2003;24:1781–5.

42. Souto EB, Wissing SA, Barbosa CM, Muller RH. Development of a controlled release formulation based on SLN and NLC for topical clotrimazole delivery. Int J Pharm. 2004;278:71–7.

43. Huang Z, Hu S, Yang Y, Fang J. Development and evaluation of lipid nanoparticles for camptothecin delivery: a comparison of solid lipid nanoparticles, nanostructured lipid carriers, and lipid emulsion. Acta Pharmacol Sin. 2008;29:1094–102.

44. Zimmermann E, Muller RH. Electrolyte and pH stabilities of aqueous solid lipid nanoparticle (SLN™) dispersions in artificial gastrointestinal media. Eur J Pharm Biopharm. 2001;52:203–10.

45. Sheikh FA, Barakat NAM, Kanjwal MA, Aryal S, Khil MS, Kim HY. Novel self-assembled amphiphilic poly (ε-caprolactone)-grafted poly (vinyl alcohol) nanoparticles: hydrophobic and hydrophilic drugs carrier nanoparticles. J Mater Sci Mater Med. 2009;20:821–31.

46. Chen CC, Tsai TH, Huang ZR, Fang JY. Effects of lipophilic emulsifiers on the oral administration of lovastatin from nanostructured lipid carriers: physicochemical characterization and pharmacokinetics. Eur J Pharm Biopharm. 2010;74:474–82.

47. Bhaskar K, Mohan CK, Lingam M, Mohan SJ, Venkateswarlu V, Rao YM. Development of SLN and NLC enriched hydrogels for transdermal delivery of nitrendipine: *in vitro* and *in vivo* characteristics. Drug Dev Ind Pharm. 2009;35:98–113.

48. Liu J, Hu W, Chen H, Ni Q, Xu H, Yang X. Isotretinoin-loaded solid lipid nanoparticles with skin targeting for topical delivery. Int J Pharm. 2007;328:191–5.

49. Joshi M, Patravale V. Formulation and evaluation of nanostructured lipid carrier (NLC)–based gel of Valdecoxib. Drug Dev Ind Pharm. 2006;32:911–8.

50. Xia Q, Saupe A, Muller RH, Souto EB. Nanostructured lipid carriers as novel carrier for sunscreen formulations. Int J Cosmet Sci. 2007;29:473–82.

51. Wissing SA, Muller RH. A novel sunscreen system based on tocopherol acetate incorporated into solid lipid nanoparticles. Int J Cosmet Sci. 2001;23:233–43.

52. Hommoss A. Nanostructured lipid carriers (NLC) in dermal and personal care formulations, Inaugural-Dissertation to obtain the academic degree Doctor rerum naturalium (Dr. rer. nat.) PhD Thesis. Free University Berlin; Germany; 2009

53. Villalobos-Hernandez JR, Muller-Goymann CC. Sun protection enhancement of titanium dioxide crystals by the use of carnauba wax nanoparticles: the synergistic interaction between organic and inorganic sunscreens at nanoscale. Int J Pharm. 2006;322:161–70.

54. Anderson MW, Hewitt JP, Spruce SR. Broad-spectrum physical sunscreens: titanium dioxide and zinc dioxide. In: Lowe NJ, Shaath NA, Pathak MA, editors. General principles in sunscreens: development, evaluation and regulatory aspects. New York: Marcel Dekker, Inc; 1997. p. 353–98.